

## Uppsala University

This is an accepted version of a paper published in *Physical Review Letters*. This paper has been peer-reviewed but does not include the final publisher proof-corrections or journal pagination.

Citation for the published paper:

Singh, B., Liu, Z., Wadsworth, R., Grawe, H., Brock, T. et al. (2011)

"16(+) Spin-Gap Isomer in (96)Cd"

*Physical Review Letters*, 107(17): 172502

Access to the published version may require subscription.

DOI: 10.1103/PhysRevLett.107.172502

Permanent link to this version:

<http://urn.kb.se/resolve?urn=urn:nbn:se:uu:diva-161938>

DiVA 

<http://uu.diva-portal.org>

# The $16^+$ spin-gap isomer in $^{96}\text{Cd}$

B.S. Nara Singh<sup>1</sup>, Z. Liu<sup>2</sup>, R. Wadsworth<sup>1</sup>, H. Grawe<sup>3</sup>, T.S. Brock<sup>1</sup>, P. Boutachkov<sup>3</sup>,  
N. Braun<sup>4</sup>, A. Blazhev<sup>4</sup>, M. Górska<sup>3</sup>, S. Pietri<sup>3</sup>, D. Rudolph<sup>5</sup>, C. Domingo-Pardo<sup>3</sup>,  
S.J. Steer<sup>6</sup>, A. Ataç<sup>7</sup>, L. Bettermann<sup>4</sup>, L. Cáceres<sup>3</sup>, K. Eppinger<sup>8</sup>, T. Engert<sup>3</sup>,  
T. Faestermann<sup>8</sup>, F. Farinon<sup>3</sup>, F. Finke<sup>4</sup>, K. Geibel<sup>4</sup>, J. Gerl<sup>3</sup>, R. Gernhäuser<sup>8</sup>,  
N. Goel<sup>3</sup>, A. Gottardo<sup>2</sup>, J. Grębosz<sup>9</sup>, C. Hinke<sup>8</sup>, R. Hoischen<sup>3,5</sup>, G. Ilie<sup>4</sup>,  
H. Iwasaki<sup>4</sup>, J. Jolie<sup>4</sup>, A. Kaşkaş<sup>7</sup>, I. Kojouharov<sup>3</sup>, R. Krücken<sup>8</sup>, N. Kurz<sup>3</sup>,  
E. Merchán<sup>3</sup>, C. Nociforo<sup>3</sup>, J. Nyberg<sup>10</sup>, M. Pfützner<sup>11</sup>, A. Prochazka<sup>3</sup>,  
Zs. Podolyák<sup>6</sup>, P.H. Regan<sup>6</sup>, P. Reiter<sup>4</sup>, S. Rinta-Antila<sup>12</sup>, C. Scholl<sup>4</sup>, H. Schaffner<sup>3</sup>,  
P.-A. Söderström<sup>10</sup>, N. Warr<sup>4</sup>, H. Weick<sup>3</sup>, H.-J. Wollersheim<sup>3</sup>, P.J. Woods<sup>2</sup>,  
F. Nowacki<sup>13</sup> and K. Sieja<sup>13</sup>

<sup>1</sup>*Department of Physics, University of York, Heslington, York, YO10 5DD, UK*

<sup>2</sup>*School of Physics and Astronomy,  
University of Edinburgh, Edinburgh, UK*

<sup>3</sup>*GSI Helmholtzzentrum für Schwerionenforschung, D-64291 Darmstadt, Germany*

<sup>4</sup>*IKP, Universität Köln, D-50937 Köln, Germany*

<sup>5</sup>*Department of Physics, Lund University, S-22100 Lund, Sweden*

<sup>6</sup>*Department of Physics, University of Surrey, Guildford, GU2 7XH, UK*

<sup>7</sup>*Department of Physics, Ankara University, 06100 Tandoğan, Ankara, Turkey*

<sup>8</sup>*Physik Department E12, Technische Universität München, D-85748 Garching, Germany*

<sup>9</sup>*The Institute of Nuclear Physics PAN, Kraków, Poland*

<sup>10</sup>*Department of Physics and Astronomy,  
Uppsala University, SE-75120 Uppsala, Sweden*

<sup>11</sup>*Faculty of Physics, University of Warsaw, PL-00-681 Warsaw, Poland*

<sup>12</sup>*Department of Physics, Oliver Lodge Laboratory,  
University of Liverpool, Liverpool, UK and*

<sup>13</sup>*IPHC, IN2P3-CNRS et Université de Strasbourg, F-67037 Strasbourg, France*

(Dated: September 16, 2011)

## Abstract

A  $\beta$ -decaying high-spin isomer in  $^{96}\text{Cd}$ , with a half-life  $T_{1/2} = 0.29^{+0.11}_{-0.10}$  s, has been established in a stopped beam Rare Isotope Spectroscopic INvestigations at GSI (RISING) experiment. The nuclei were produced using the fragmentation of a primary beam of  $^{124}\text{Xe}$  on a  $^9\text{Be}$  target. From the half-life and the observed  $\gamma$  decays in the daughter nucleus,  $^{96}\text{Ag}$ , we conclude that the  $\beta$ -decaying state is the long predicted  $16^+$  “spin-gap” isomer. Shell-model calculations, using the Gross-Frenkel interaction and the  $\pi\nu(p_{1/2}, g_{9/2})$  model space, show that the iso-scalar component of the neutron-proton interaction is essential to explain the origin of the isomer. Core excitations across the  $N = Z = 50$  gaps and the Gamow-Teller strength,  $B(GT)$  distributions have been studied via large-scale shell-model calculations using the  $\pi\nu(g, d, s)$  model space to compare with the experimental  $B(GT)$  value obtained from the half-life of the isomer.

PACS numbers: PACS 21.60.Cs, 23.35.+g, 23.20.Lv, 26.20.-f

The nuclear landscape around the heaviest known bound doubly-magic self-conjugate nucleus  $^{100}\text{Sn}$ , which resides far from the valley of stability, exhibits a rich variety of nuclear structure phenomena [1–15]. A feature of great interest in this region is the presence of isomeric states, especially those which may undergo particle decay. Indeed, early work by Peker *et al.* was paramount in motivating studies of such states based on three or four particle/hole configurations in nuclei. This included the  $16^+$  isomeric state in  $^{96}\text{Cd}$ , which was suggested to result from a four-hole configuration relative to a  $^{100}\text{Sn}$  core that may decay via proton radioactivity [1].

A particularly interesting issue in this region is the role played by the neutron-proton,  $np$ , interaction in leading to the existence of the isomers. The iso-vector ( $T = 1$ ) component of the interaction between like-nucleons is known to dominate in all non-self-conjugate nuclei whilst the  $T = 1$   $np$  interaction has been shown to have a major influence on the  $N = Z$  line below mass 80 due to the large overlap of the proton and neutron wave-functions [16]. Although calculations suggest an important influence of the iso-scalar ( $T = 0$ )  $np$  interaction on the structure of medium-heavy  $N = Z$  nuclei, its role has been less clear and often debated [17–20]. Very recent experimental work has claimed the first indications for the crucial role of this interaction at low-spins in  $^{92}\text{Pd}$ , that are supported by shell-model (SM) calculations [2]. In order to establish or dispute the expected strong influence of the  $T = 0$   $np$  interaction for self-conjugate nuclei close to  $^{100}\text{Sn}$ , it is of paramount importance to obtain further evidence for its effects.

Long standing SM calculations for the self-conjugate nucleus  $^{96}\text{Cd}$  predict the presence of a  $16^+$  state at an energy lower than that of the first  $12^+$  and  $14^+$  states [10]. This situation arises from the strong influence of the  $T = 0$   $np$  interaction and results in “spin-gap” isomerism [4] for the  $16^+$  state, since its  $E6$   $\gamma$  decay to the next available  $10^+$  state is highly hindered. Consequently,  $\beta^-$ ,  $\beta^-$ -delayed proton and proton decays may be expected to become favorable modes of de-excitation [1, 10]. The identification of such decay characteristics, along with the evolution of single-particle energies, provides a sensitive probe of the residual interactions seen by the nucleons and can serve as critical tests of nuclear models. Studies related to the predicted “spin-gap” isomerism in  $N \approx Z \approx 50$  nuclei around the proton drip line also have been of great interest due to the purity of the wave-functions and the possibility to describe their properties using only a few orbitals [4–7, 21]. Apart from providing important data on the  $np$  interaction, the structural properties of these nuclei

also serve as key inputs to the astrophysical  $rp$ -process calculations [22].

In this Letter, we report on the identification of an isomeric state in  $^{96}\text{Cd}$  that  $\beta$  decays mainly to the  $(15^+)$  isomeric state in  $^{96}\text{Ag}$  [21]. From the observed Gamow-Teller (GT) strength and the decay  $\gamma$  rays, we conclude that this provides evidence for the existence of the long predicted  $16^+$  “spin-gap” isomer in  $^{96}\text{Cd}$  [10]. This is the second highest spin (the  $21^+$  isomeric state in  $^{94}\text{Ag}$  being the highest [3]) observed for a state preceding  $\beta$  decay.

$^{96}\text{Cd}$  nuclei were produced at GSI by fragmentation of an 850 MeV/u  $^{124}\text{Xe}$  primary beam with an intensity of  $10^9$  particles/second from the SIS-18 synchrotron on a  $4g/cm^2$   $^9\text{Be}$  target. The nuclei of interest were separated using the FRagment Separator (FRS) [23] and transported to its  $S4$  focal plane, where the RISING [24, 25] stopped beam setup was located. The ions, fully stripped ( $Q = Z$ ) due to their relativistic energies, were identified on an event-by-event basis [21, 23–25]. Fig. 1 shows the  $Z$  versus  $A/Q$  identification plot for the implanted ions. Here,  $A$ ,  $Q$  and  $Z$  are the mass, charge state and the atomic number of the fragments, respectively.

The  $^{96}\text{Cd}$  nuclei were slowed down using an aluminium degrader at the  $S4$  focal plane. Subsequently, the ions were stopped in an ‘active stopper’ (AS) that detected the implantation position of nuclei as well as the particles from their decays [26]. The AS consisted of nine double sided silicon strip detectors (DSSSD) arranged in three horizontal rows perpendicular to the beam direction, with three detectors in each row. Each DSSSD was 1 mm thick with an area of  $5 \times 5 \text{ cm}^2$  and had 16  $X$ - and 16  $Y$ -strips [27]. This geometrical arrangement also had an optimal solid angle coverage for the decays from the nuclei implanted in the central detector. The primary beam and FRS settings were optimized so as to stop the  $^{96}\text{Cd}$  nuclei in the center of the AS. To detect the  $\gamma$  rays from the fragments, the AS was surrounded by 15 EUROBALL cluster detectors, each cluster comprising seven individual HPGe crystals. A timing signal from a scintillator placed down-stream to the  $S4$  focal plane, corresponding to the instance of fragment implantation (see [24, 28] for details), was used for time correlations with subsequent decays.

A total of 630  $^{96}\text{Cd}$  nuclei were identified by the FRS focal plane detectors in the current experiment in a period of close to 8 days. In the analysis presented here, we used approximately 95% of these events that were implanted into the detector located in the middle of the AS. The end-point energies, for the  $\beta$  decay of the ground and  $16^+$  states in  $^{96}\text{Cd}$ , are expected to be in the range of 8 to 10 MeV [29, 30] and most of the resulting  $\beta$  particles are

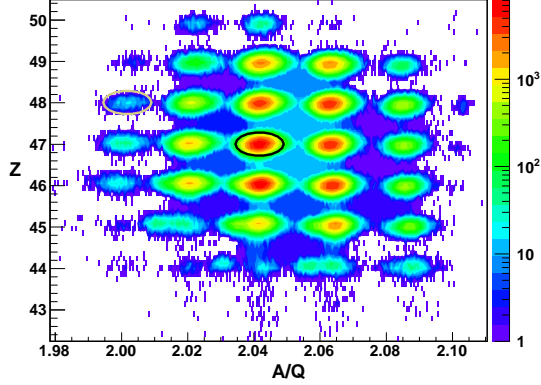


FIG. 1: (Color online)  $Z$  versus  $A/Q$  identification plot.  $^{96}_{48}\text{Cd}$  and  $^{96}_{47}\text{Ag}$  nuclei are circled. estimated to deposit an energy of up to 600 keV in a single strip of a Si detector. Fig. 2(a) shows the prompt  $\gamma$ -ray events which follow within a time window of up to 200 ns after a  $\beta$ -decay event, that deposited an energy of up to  $\simeq 600$  keV in the AS and has been identified within a correlation time of up to one second after  $^{96}\text{Cd}$  implantation. The latter are defined by a contour line in Fig. 1. A  $\gamma$  ray at 421 keV is observed, next to the dominant 511 keV line arising from positron annihilation.

SM calculations for  $^{96}\text{Ag}$ , using the Gross-Frenkel (GF) interaction and the  $\pi\nu(p_{1/2}, g_{9/2})$  model space, predict the lowest  $1^+$  and  $2^+$  states at excitation energies of 356 keV and 12 keV, respectively, above an  $8^+$  ground state [31]. Experimentally, spins/parities of  $2^+$ ,  $8^+$  have been tentatively assigned to two low-lying states based on the  $\beta^+/\text{EC}$  decay [32, 33]. Low-lying  $1^+$  states of odd-odd  $N = 49$  isotones are populated in  $\beta^+/\text{EC}$  GT decay from the ground states of their even-even neighbours and are connected to the  $2^+$  states by  $M1$  transitions [34]. Therefore, we tentatively assign the observed 421 keV  $\gamma$  line to a  $(1^+) \rightarrow (2^+)$  transition in  $^{96}\text{Ag}$  fed by  $\beta^+/\text{EC}$  decay of the  $^{96}\text{Cd}$  ground state (see Fig. 3). The time distribution of the 421 keV  $\gamma$  ray with respect to the implantation of  $^{96}\text{Cd}$  is shown in the inset of Fig. 2(a). An analysis based on the maximum likelihood method yields  $T_{1/2} = 0.67 \pm 0.15$  s. This is in good agreement with the known value of  $1.03^{+0.24}_{-0.21}$  s reported for the ground state decay of  $^{96}\text{Cd}$  [8]. From the observed  $\gamma$  intensities in Fig. 2(a), we estimate an upper limit of 10% population for the  $16^+$  isomeric state implying  $\sim 90\%$  population for the ground state. This ‘isomeric ratio’ is similar to that observed for the  $15^+$  isomeric state in  $^{96}\text{Ag}$ , but somewhat higher than our theoretical estimation of  $\sim 2\%$  [21, 35].

Fig. 2(b) shows the  $\gamma$ -ray spectrum that was obtained with the same conditions as those for Fig. 2(a), except that the events are delayed by 200 ns to 4  $\mu\text{s}$  with respect to the  $\beta$ -decay

signal. In this case there is evidence for  $\gamma$  rays at 470, 667 and 1506 keV, two of which were first observed by Gryzwacz et al. [36]. These are identical to the main observed transitions following the decay of the ( $15^+$ ) isomer in  $^{96}\text{Ag}$  (see Fig. 3), which has  $T_{1/2} = 1.5 \mu\text{s}$  [21, 37] - a value which is about twice that inferred in Ref. [36]. To investigate other possible contributions from random coincidences Fig. 2(c), using the same conditions as those for Fig. 2(b), shows  $\gamma$  rays which are in coincidence with all fragments other than  $^{96}\text{Cd}$  that are stopped in the central detector. This spectrum shows no evidence for the 470, 667 or 1506 keV  $\gamma$ -ray lines. We therefore conclude that the  $\gamma$  rays observed in Fig. 2(b) result directly from the  $\beta$  decay of the  $16^+$  “spin-gap” isomer in  $^{96}\text{Cd}$ , since  $\beta$ -decay selection rules for GT decays ( $\Delta I = 0, 1$ ) exclude the possibility of the  $0^+$  ground state in  $^{96}\text{Cd}$  populating such a high-spin isomer in its daughter  $^{96}\text{Ag}$ . The extracted time distribution of the  $\beta$ -decay events when the three  $\gamma$  decays are simultaneously detected is shown in the inset to Fig 2(b). The maximum likelihood method gives  $T_{1/2} = 0.29^{+0.11}_{-0.10}$  s for the distribution. This is in good agreement, within the uncertainties, with the expected value of 0.5 s from Ref. [10] for the GT decay of the  $16^+$  “spin-gap” isomer.

Fig. 3 (left column) shows the results of SM calculations for  $^{96}\text{Cd}$  using the GF interaction and the  $\pi\nu(p_{1/2}, g_{9/2})$  model space [31]. Further details on our SM approach can be found in Refs. [7, 21]. The  $16^+$  isomer has a  $\pi\nu(p_{1/2}^2 g_{9/2}^8)$  particle configuration within  $\pi\nu(p_{1/2}, g_{9/2})$  model space, leaving two proton ( $\pi(g_{9/2}^{-2})$ ) and two neutron ( $\nu(g_{9/2}^{-2})$ ) holes coupled to the maximum possible spin  $I = 16$ .

Fig. 3 (center) shows the results of our SM calculations performed with either the  $T = 0$  or  $T = 1$   $np$  interaction switched off. Here, the original proton and neutron particle/hole energies for both,  $^{88}\text{Sr}$  and  $^{100}\text{Sn}$  are maintained by using a monopole correction [38]. The  $16^+$  state moves up substantially to lie above the  $12^+$  and  $14^+$  states and no longer forms a “spin-gap” isomer when the  $T = 0$   $np$  interaction is switched off. Our identification of the  $16^+$   $\beta$ -decaying isomer therefore provides additional evidence for the importance of the  $T = 0$   $np$  interaction at high-spins in  $A \simeq 90$ -100  $N = Z$  nuclei.

The  $15^+$  isomeric state in  $^{96}\text{Ag}$  (c.f. Fig. 3) has a pure  $\pi\nu(p_{1/2}^2)\pi(g_{9/2}^7)\nu(g_{9/2}^9)$  configuration within the  $\pi\nu(p_{1/2}, g_{9/2})$  model space with the  $\pi(g_{9/2}^{-3})\nu(g_{9/2}^{-1})$  holes coupled to the maximum possible spin [21]. This scenario results in the full GT strength for a  $g_{9/2}$  proton (projection  $5/2$ )  $\rightarrow$   $g_{9/2}$  neutron (projection  $7/2$ ) transition that is illustrated schematically in Fig. 4 (left). This is similar to the decay of the  $12^+$  isomeric state in  $^{52}\text{Fe}$  to the  $11^+$  state in

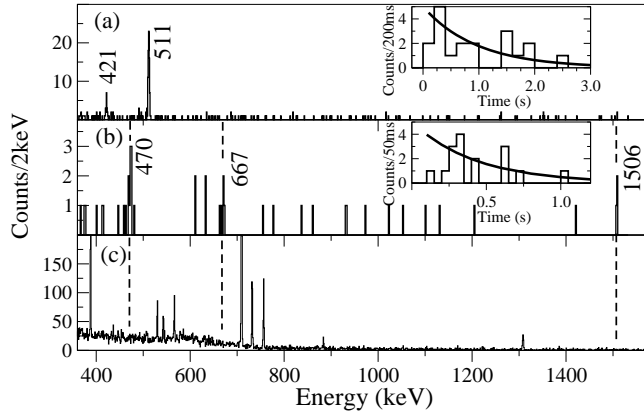


FIG. 2: Gamma-ray spectra associated with the decays following implantation into the geometrically central DSSSD of the ‘active stopper’. a)  $^{96}\text{Cd}$  events with  $\gamma$ -ray times restricted to be between 0 to 200 ns following the  $\beta$ -decay signal detected in the DSSSD. In the inset the time distribution of the 421 keV  $\gamma$  ray with respect to the  $^{96}\text{Cd}$  implantation time is shown for the data (histogram) and the calculations (smooth curve) using  $T_{1/2} = 0.67 \pm 0.15$  s. b) Same as a) except the  $\gamma$ -ray times are restricted to be between 200 ns to 4  $\mu\text{s}$ . The inset shows the combined correlation time distribution of the 470, 667, 1506 keV  $\gamma$  rays which gives  $T_{1/2} = 0.29^{+0.11}_{-0.10}$  s for the  $16^+$  isomer. c) Same as b) for all nuclei other than  $^{96}\text{Cd}$ . In the above spectra, the 511 keV line arises from the positron annihilation whilst the remaining lines with labels correspond to the transitions in  $^{96}\text{Ag}$  (c.f. Fig. 3). See text for details. The dashed lines are merely to guide the eye to particular energy co-ordinates.

its daughter  $^{52}\text{Mn}$ , one major harmonic oscillator shell below, with a small  $B(GT)$  value of 0.061 [34, 39].

The experimental GT strength in standard units is related to the half-life via  $B(GT) = \frac{3860(18) \cdot I_\beta}{f \cdot T_{1/2}}$  [40], where  $I_\beta$  is the branching ratio and  $f$  is the phase space function tabulated for various  $Q_{EC}$  values in Ref. [41]. We obtain  $B(GT) = 0.19^{+0.10}_{-0.06}$ , using  $T_{1/2} = 0.29^{+0.11}_{-0.10}$  s, 100% for  $I_\beta$  and  $Q_{EC} = 11.51 \pm 0.26$  MeV. The latter is extrapolated from the groundstate-to-groundstate value [30] and the GF shell-model calculations. This is in good agreement with the SM result for the  $\pi\nu(p_{1/2}, g_{9/2})$  model space of  $B(GT) = 0.14$ , where we have used 0.6 for the GT quenching taken from Ref. [30].

In order to investigate the effects in an extended model space, we carried out large-scale shell-model (LSSM) calculations in a  $\pi\nu(g, d, s)$  space using a  $^{80}\text{Zr}$  core and including up to  $t=4$  ( $^{96}\text{Cd}$ ) or  $t=5$  ( $^{96}\text{Ag}$ ) particle-hole ( $ph$ ) core excitations across the  $N = Z = 50$  shell gap [5, 21]. In this case a quenching factor of 0.75 was used for the GT operator [42].

The relevant calculated level scheme for  $^{96}\text{Ag}$  is shown in the next to the last column of Fig. 3. The calculations in Fig. 4 (right) show the decay of the parent  $16^+$  state. This contains 76% content of the  $(\pi g_{9/2}^{-2} \nu g_{9/2}^{-2})_{16}$  configuration and decays to the first  $15^+$  (isomeric) state at 2.62 MeV and the  $15^+$ ,  $16^+$  and  $17^+$  GT resonance states, which have  $\simeq 2$  MeV width at centroid energies of 10.2, 10.6 and 9.5 MeV, respectively. The  $B(GT)$  values for these states are calculated to be 0.07, 2.78, 2.33 and 1.41, respectively. Clearly, in these calculations, the  $15^+$  state at 2.62 MeV is predicted to have a factor two smaller value for  $B(GT)$  compared to the GF estimate of 0.14. Both these estimates agree, within the uncertainties, with our experimental result. Future measurements with better statistics will be needed to study all the decay branches that should validate the calculations. It should be noted that the observed difference in the estimates is due to the core excitations included in LSSM calculations. A similar effect of core excitations is found for the  $^{100}\text{Sn}$  case. A large GT strength is entirely concentrated in the  $\pi(g_{9/2}) \rightarrow \nu(g_{7/2})$  transition to the  $1^+$  state in  $^{100}\text{In}$ , when no core excitations are considered. The strength to this state is reduced by 19% for SM calculations performed in the  $(g, d, s)$  space at low truncation levels,  $t=2$  for  $^{100}\text{Sn}$  and  $t=3$  for  $^{100}\text{In}$  [11]. Further reduction is anticipated from an LSSM calculation at  $t=5$  due to the fragmentation of  $B(GT)$  to several  $1^+$  states [43].

The decay energies from the  $16^+$  state to the GT resonance states in the daughter are smaller, therefore the phase space is smaller, compared to that for the  $15^+$  isomeric yrast state. Consequently, the  $15^+$  state is predicted to receive about 68% branching. The remaining 32% feeds the predicted  $15^+$ ,  $16^+$  and  $17^+$  GT resonance states, which lie at energies above the proton threshold. These are expected to decay via competing  $\beta$ -delayed proton and  $\gamma$  decays with 33 % and 67 % branching ratios, respectively. As shown in Fig. 4 (right), the latter are expected to feed the  $15^+$  state at 2.62 MeV via  $M1$  and  $E2$  transitions. However, due to the limitations in the detection efficiencies and statistics in our data, the corresponding high energy  $\gamma$  transitions could not be observed. The  $\gamma$  branch creates a pandemonium problem [44], since the non-observed feeding via  $M1$  and  $E2$  transitions (see Fig.4 (right)) to the  $15^+$  daughter state has a larger value for the  $B(GT)$  which is not accounted for in the experimental  $B(GT)$  based on the assumption of  $I_\beta=100\%$ . This warrants a caution when comparing our experimental value with the theoretical estimates for the  $B(GT)$  strength to the  $15^+$  state or for the total  $B(GT)$  strength. Future experiments with better statistics will be useful in understanding the hindrance factor in GT strengths

in this region [45].

Recent work [15] identified the  $25/2^+$  “spin-gap” isomer in  $^{97}\text{Cd}$  and pointed out that when multiple  $\beta$ -decaying states are present, the measured half-lives need to be carefully analyzed to deduce the half-life of the ground state, which is usually the important quantity for nuclear astrophysics. Bazin *et al.* reported on the decay half-life of  $^{96}\text{Cd}$  [8]. However, it was not known whether their result was for the ground state, the isomeric state, or a combination of the two states. Our work allows us to deduce  $T_{1/2} = 0.67 \pm 0.15$  s for the ground state in  $^{96}\text{Cd}$ . This value is smaller but, within the uncertainties, agrees with the result from Ref. [8] and thereby supports their conclusion that the x-ray bursters are not the main source for the large abundances of  $^{96}\text{Ru}$  in the solar system.

In summary, evidence for the existence of the  $16^+$   $E6$  “spin-gap” isomer in  $^{96}\text{Cd}$  is presented for the first time and supported by SM calculations on the level structure and GT strengths. This result provides important evidence for the strong influence of the isoscalar neutron-proton interaction not only at low-spins as in the case of  $^{92}\text{Pd}$  [2], but also at high-spin in the region around  $^{100}\text{Sn}$ .

This work has been supported by the UK STFC, the German BMBF under Contracts No. 06KY205I, No. 06KY9136I, and No. 06MT9156, the Swedish Research Council, and the DFG cluster of excellence Origin and Structure of the Universe.

- 
- [1] L.E. Peker *et al.*, Phys. Lett. B **36**, 547 (1971).
  - [2] B. Cederwall *et al.*, Nature, **469**, 68 (2011).
  - [3] I. Mukha *et al.*, Phys. Rev. Lett. **95**, 022501 (2005), Nature, **439**, 298 (2006).
  - [4] H. Grawe *et al.*, Eur. Phys. J A **27**, s01, 257 (2006).
  - [5] A. Blazhev *et al.*, Phys. Rev. C **69**, 064304 (2004).
  - [6] M. Górska *et al.*, Phys. Rev. Lett. **79**, 2415 (1997).
  - [7] T. S. Brock *et al.*, Phys. Rev. C **82**, 061309(R) (2010).
  - [8] D. Bazin *et al.*, Phys. Rev. Lett. **101**, 252501 (2008).
  - [9] I.G. Darby *et al.*, Phys. Rev. Lett. **105**, 162502 (2010).
  - [10] K. Ogawa, Phys. Rev. C **28**, 958 (1983).
  - [11] B.A. Brown and K. Rykaczewski, Phys. Rev. C **50**, 2270(R) (1994).

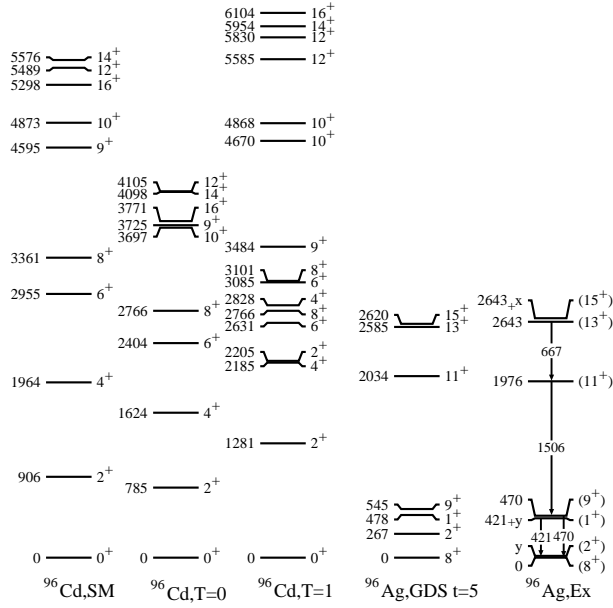


FIG. 3: Shell-model calculations for  $^{96}\text{Cd}$ .  $^{96}\text{Cd,SM}$ : All iso-vector  $nn$ ,  $pp$ ,  $np$  and iso-scalar  $np$  interactions are included.  $^{96}\text{Cd,T} = 0$ : Only the iso-vector  $np$  interaction is switched off.  $^{96}\text{Cd,T} = 1$ : Only the iso-scalar  $np$  interaction is switched off. Large-scale shell-model calculations for  $^{96}\text{Ag}$ .  $^{96}\text{Ag,GDS } t=5$ : Up to 5  $ph$  core excitations across the  $N = Z = 50$  shell gap are included. Only the lowest states are shown for each spin. EX: Partial experimental scheme and the transitions observed in the decay of  $^{96}\text{Cd}$  [21, 37]. Here, x and y correspond to the unobserved transition energies.

[12] A. Juodagalvis and D. J. Dean, Phys. Rev. C **72**, 024306 (2005).

[13] M. Honma *et al.*, Phys. Rev. C **80**, 064323 (2009).

[14] S. Zerguine and P. Van Isacker, Phys. Rev. C **83**, 064313 (2011).

[15] G. Lorusso *et al.*, Phys. Lett. B **699**, 141 (2011).

[16] A. Afanasjev and S. Frauendorf, Phys. Rev. C **71**, 064318 (2005) and the references therein.

[17] J. Engel *et al.*, Phys. Lett. B **389**, 211 (1996).

[18] A.L. Goodman, Adv. Nucl. Phys. **11**, 263 (1979) and Phys. Rev. C **60**, 014311 (1999).

[19] W. Satula and R. Wyss, Phys. Lett. B **393**, 1 (1997) and Phys. Rev. Lett. **86**, 4488 (2001).

[20] E. Caurier *et al.*, Phys. Rev. C **82**, 064304 (2010).

[21] P. Boutachkov *et al.*, Phys. Rev. C **84**, in print (2011).

[22] H. Schatz *et al.*, Phys. Rep. **294**, 167 (1998).

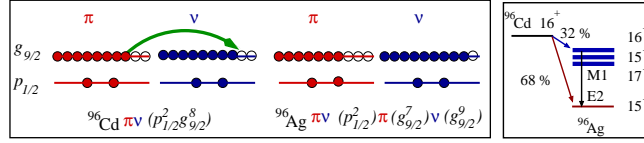


FIG. 4: (Color online) Left: The proton and neutron occupations lined up in the sequence of increasing projection in the  $p_{1/2}$  and  $g_{9/2}$  orbitals representing the  $16^+$  “spin-gap” isomer in  $^{96}\text{Cd}$  and the  $15^+$  isomer in  $^{96}\text{Ag}$  [21]. The GT  $\beta$ -decay process ( $\pi g_{9/2} \rightarrow \nu g_{9/2}$ ) is depicted by the arrow that receives the full GT strength within the  $\pi\nu(p_{1/2}, g_{9/2})$  space. Right: Decay branches are shown from the large-scale shell-model calculations with core excitations allowing different transitions including the one depicted on the left. Overlaps of the resonances, due to their  $\simeq 2$  MeV width, are not shown for the clarity. See text for details.

- [23] H. Geissel, Nucl. Instrum. Meth. B **70**, 286 (1992).
- [24] D. Rudolph *et al.*, Eur. Phys. J **150**, 173 (2007) and D. Rudolph, Acta Phys. Pol. **42**, 567 (2011).
- [25] H.-J. Wollersheim *et al.*, Nucl. Instr. Meth. A **537**, 637 (2005), S. Pietri *et al.*, Nucl. Instr. Meth. A **261**, 1079 (2007).
- [26] Zs. Podolyak *et al.*, Phys. Lett. B, **672**, 116 (2009).
- [27] R. Kumar *et al.*, Nucl. Instrum. Meth. A **598**, 754 (2009), N. Alkhomashi *et al.*, Phys. Rev. C **80**, 064308 (2009).
- [28] S. Pietri *et al.*, Eur. Phys. J **150**, 319 (2007).
- [29] G.T. Biehle and P. Vogel, Phys. Rev. C **46**, 1555 (1992).
- [30] H. Herndl and B.A. Brown, Nucl. Phys. **A627**, 35 (1997).
- [31] R. Gross and A. Frenkel, Nucl. Phys. **A267**, 85 (1976).
- [32] W. Kurcewicz *et al.*, Z Phys. **A308**, 21 (1982).
- [33] L. Batist *et al.*, Nucl.Phys. **A720**, 245 (2003).
- [34] ENSDF database, <http://www.nndc.bnl.gov/ensdf/>.
- [35] M. Pfützner *et al.*, Phys. Rev. C **65**, 064604 (2002).
- [36] R. Grzywacz *et al.*, Phys. Rev. C **55**, 1126 (1997).
- [37] A. D. Becerril *et al.*, Phys. Rev. C **84**, (R), in print.
- [38] H. Grawe *et al.*, Rep. Progr. Phys. **70**, 1525 (2007).
- [39] D.F. Geesaman *et al.*, Phys. Rev. Lett. **34**, 326 (1975), Phys. Rev. C **19**, 1938 (1979).

- [40] A. Plochoki *et al.*, Z Phys. **A342**, 43 (1992).
- [41] N.B. Gove and M.J. Martin, Nucl. Data Tab. **A10**, 205 (1971).
- [42] E. Caurier *et al.*, Rev. Mod. Phys. **77**, 427 (2005).
- [43] Ch. Hinke *et al.*, to be published and K. Sieja, private communication.
- [44] J.C. Hardy *et al.*, Phys. Lett. **71**, 307 (1977).
- [45] I.S. Towner, Nucl. Phys. **A444**, 402 (1985).